

FancyVideo: Towards Dynamic and Consistent Video Generation via Cross-frame Textual Guidance

Jiasong Feng^{1*}, Ao Ma^{1*}, Jing Wang^{1,2*}, Bo Cheng¹, Xiaodan Liang², Dawei Leng^{1†}, Yuhui Yin¹,

¹360 AI Research ²Sun Yat-sen University
fengjiasong@360.cn mao@360.cn wangj977@mail2.sysu.edu.cn

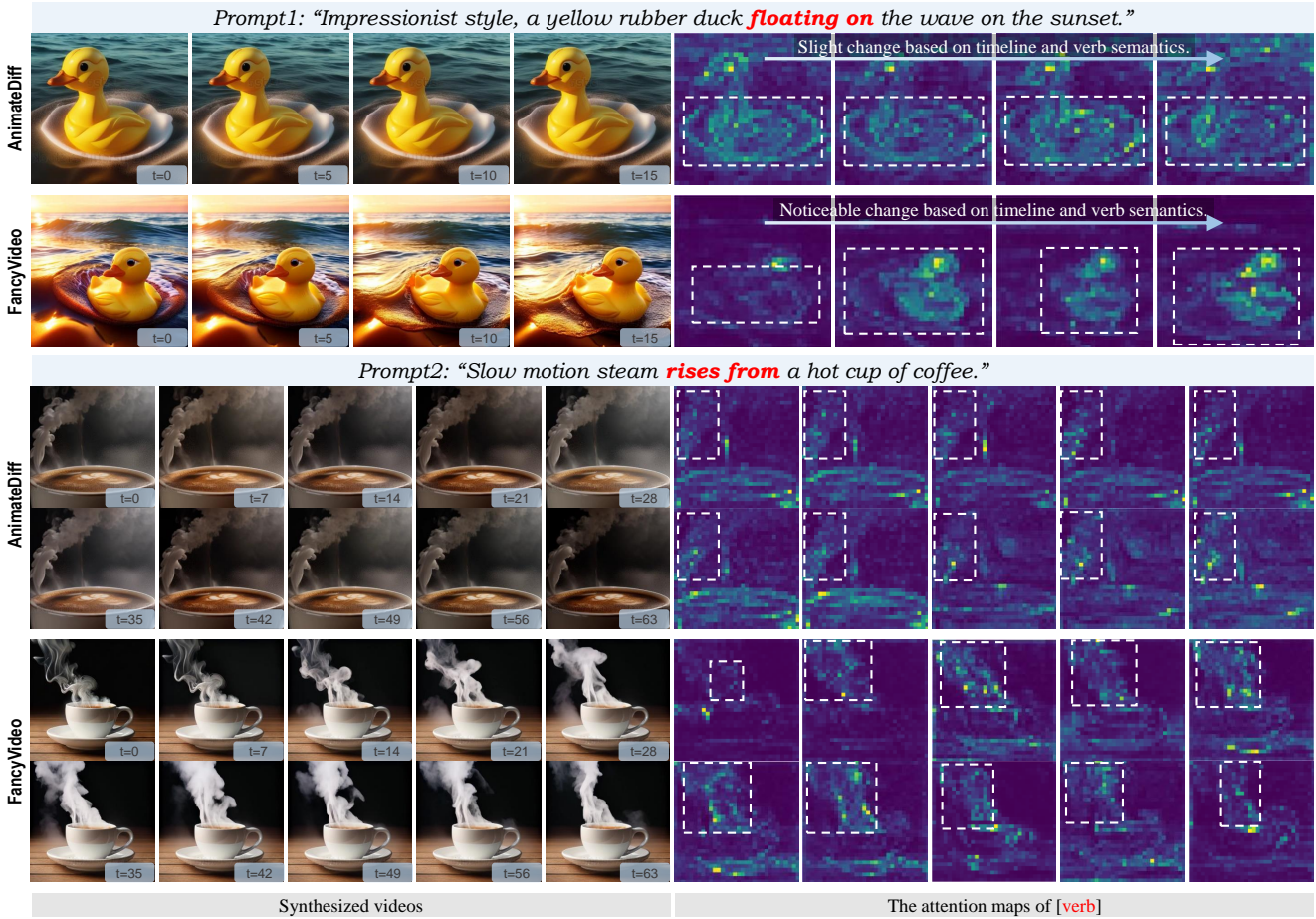


Figure 1: **The generated videos and the attention maps of [verb] belong to FancyVideo and AnimateDiff.** We present the 16-frame video (top) and longer 64-frame video (bottom). Due to the inadequate time-specific textual guidance in the AnimateDiff, the [verb] focused region remains almost constant, resulting in a lack of motion in the video. In contrast, **FancyVideo** effectively alleviates this issue through cross-frame textual guidance. The [verb] focused region changes based on the timeline and semantics, thereby generating motion-rich videos.

Abstract

Synthesizing motion-rich and temporally consistent videos remains a challenge in artificial intelligence, especially when dealing with extended durations. Existing text-to-video (T2V) models commonly employ spatial cross-attention for text control, equivalently guiding different frame generations without frame-specific textual guidance. Thus, the model’s

capacity to comprehend the temporal logic conveyed in prompts and generate videos with coherent motion is restricted. To tackle this limitation, we introduce **FancyVideo**, an innovative video generator that improves the existing text-control mechanism with the well-designed **Cross-frame Textual Guidance Module (CTGM)**. Specifically, CTGM incorporates the **Temporal Information Injector (TII)**, **Temporal Affinity Refiner (TAR)**, and **Temporal Feature Booster (TFB)** at the beginning, middle, and end of cross-attention, respectively, to achieve frame-specific textual guidance. Firstly, TII

*These authors contributed equally.

†Corresponding Authors.

injects frame-specific information from latent features into text conditions, thereby obtaining cross-frame textual conditions. Then, TAR refines the correlation matrix between cross-frame textual conditions and latent features along the time dimension. Lastly, TFB boosts the temporal consistency of latent features. Extensive experiments comprising both quantitative and qualitative evaluations demonstrate the effectiveness of FancyVideo. Our approach achieves state-of-the-art T2V generation results on the EvalCrafter benchmark and facilitates the synthesis of dynamic and consistent videos. Our video demo, code and model are available at <https://360cvgroup.github.io/FancyVideo/>.

Introduction

With the advancement of the diffusion model, the text-to-image (T2I) generative models (Blattmann et al. 2023b; Ge et al. 2023; Ho et al. 2022; Luo et al. 2023) can produce high-resolution and photo-realistic images by complex text prompts, resulting in various applications. Currently, many studies (Yu et al. 2023; Guo et al. 2023a; Wang et al. 2024; Zhou et al. 2022) explore the text-to-video (T2V) generative model due to the great success of T2I models. However, building a powerful T2V model remains challenging as it requires maintaining temporal consistency while generating coherent motions simultaneously. Moreover, due to limited memory, most diffusion-based T2V models (Yu et al. 2023; Guo et al. 2023a; Zhang et al. 2024; Guo et al. 2023b; Chen et al. 2023; Menapace et al. 2024; Wang et al. 2023b) can only produce fewer than 16 frames of video per sampling without extra assistance (i.e., super-resolution).

The existing T2V models (Zhang et al. 2024; Guo et al. 2023b; Chen et al. 2023; Menapace et al. 2024; Wang et al. 2023b) typically employ spatial cross-attention between text conditions and latent features for achieving text control generation. However, as shown in Fig. 2(I), this manner shares the same text condition across different frames, thus lacking the specific textual guidance tailored to each frame. Consequently, these T2V models struggle to comprehend the temporal logic of text prompts and produce videos with coherent motion. Taking AnimateDiff (Guo et al. 2023b) as an example, in Fig. 1, we exhibit its generated video and visualize the [verb]-focused region (which is closely associated with the video motion) based on the attention map from the cross-attention module. Ideally, these regions should transition smoothly over time and align with the semantics of motion instructions. However, as observed in the upper right of the figure, the [verb]-focused region remains nearly identical across different frames due to the consistent textual guidance between frames. Meanwhile, the video exhibits poor motion in the upper left of the figure. Furthermore, we perform a similar visual analysis for the longer video (e.g., 64 frames) generation and find that this problem is more prominent, as illustrated in the lower part of Fig. 1. Therefore, we believe this approach hampers the advancement of video dynamics and consistency and is sub-optimal for video generation tasks based on text prompts.

To this end, we present a novel T2V model named **FancyVideo**, capable of comprehending complex spatial-temporal relationships within text prompts. By employing a cross-frame textual guidance strategy, FancyVideo can gen-

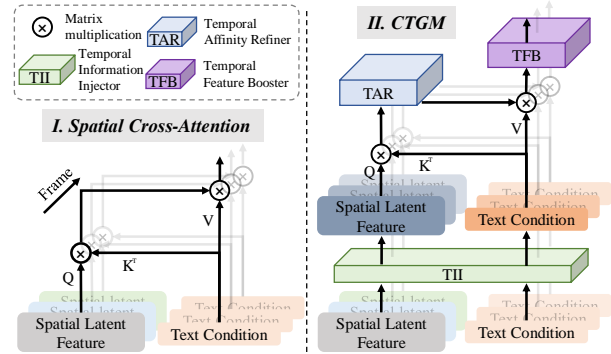


Figure 2: The structure of spatial cross-attention and CTGM.

erate more dynamic and plausible videos in a sampling process. Specifically, to boost the model’s capacity for understanding spatial-temporal information in text prompts, we optimize the spatial cross-attention through the proposed Cross-frame Textual Guidance Module (CTGM), comprising a Temporal Information Injector (TII), Temporal Affinity Refiner (TAR), and Temporal Feature Booster (TFB). As illustrated in Fig. 2(II), TII injects temporal information from latent features into text conditions, building cross-frame textual conditions. Then, TAR refines the affinity between frame-specific text embedding and video along time dimension, adjusting the temporal logic of textual guidance. Lastly, TFB further boosts the temporal consistency of latent features. Through the cooperative interaction between TII, TAR, and TFB, FancyVideo fully captures the motion logic embedded within images and text. Consequently, its motion token-focused area shifts logically with frames, as illustrated in the lower right part of Fig. 1. This characteristic enables FancyVideo to produce dynamic videos, as displayed in the lower left part of the figure. Experiments demonstrate that FancyVideo successfully generates dynamic and consistent videos, achieving the SOTA results on the EvalCrafter (Liu et al. 2023) benchmark and the competitive performance on UCF-101 (Soomro, Zamir, and Shah 2012) and MSR-VTT (Xu et al. 2016).

Contributions. **1)** We introduce FancyVideo, the pioneering endeavor as far as our knowledge extends, delving into cross-frame textual guidance for the T2V task. This approach offers a fresh perspective to enhance current text-control methodologies. **2)** We propose the Cross-frame Textual Guidance Module (CTGM), which constructs cross-frame textual conditions and subsequently guides the modeling of latent features with robust temporal plausibility. It can effectively enhance the motion and consistency of video. **3)** We demonstrate that incorporating cross-frame textual guidance represents an effective approach for achieving high-quality video generation. Our experiments showcase that this approach attains state-of-the-art results on both quantitative and qualitative evaluations.

Related Work

Text to Video Generation. Research in this field has employed various generative models, including GANs (Zhu et al. 2017; Wang et al. 2020; Munoz et al. 2021; Gur, Benaim, and Wolf 2020), auto-regressive models (Wang et al.

2019; Ramesh et al. 2021; Yan et al. 2021; Razavi, Van den Oord, and Vinyals 2019), and implicit neural representations (De Luigi et al. 2023). Recently, diffusion models (Zhang, Rao, and Agrawala 2023; Rombach et al. 2022; Zhang et al. 2023a; Ruiz et al. 2023) have advanced text-to-image generation quality, outperforming previous techniques. Stable Diffusion (Rombach et al. 2022) adapts the diffusion process to VAE’s (Kingma and Welling 2013) latent space, reducing computation and memory requirements. Inspired by T2I success, T2V studies (Ren et al. 2024; Jiang et al. 2023; Xing et al. 2024; Wu et al. 2023a) add temporal layers to pre-trained T2I models to capture temporal information while reducing video generation costs. However, these methods often use a single text condition for spatial cross-attention, leading to inconsistent temporal context across frames and affecting motion coherence. Our work introduces a cross-frame textual guidance mechanism to tailor temporal context for each frame, generating more realistic and temporally consistent videos.

Image-conditioned Video Generation. The gap between text prompts and videos has steered research towards using images for clearer video generation. SVD (Blattmann et al. 2023a) uses images as noisy latent variables for frame generation, while MoonShot (Zhang et al. 2024) enhances semantic consistency through the CLIP encoder. These I2V methods require specific input images. Hierarchical approaches (Zeng et al. 2023; Chen et al. 2023) use images as key frames, potentially creating lengthy videos with fewer image constraints. These methods, essentially T2V, also support I2V. FancyVideo, a hierarchical method with cross-frame textual guidance, generates more frames per iteration, cutting down inference time.

Method

Preliminaries

Latent Diffusion Models. The latent diffusion models (LDMs) (Sohl-Dickstein et al. 2015; Ho, Jain, and Abbeel 2020) are a class of efficient diffusion models that convert the denoising process into the compressed latent space instead of the pixel space. Specifically, LDMs employ VAE’s (Kingma and Welling 2013) encoder to compress the image into latent code and learn the data distribution by performing a forward and inverse diffusion process on the latent code. It assumes a forward process that gradually introduces the gaussian noise ($\epsilon \sim \mathcal{N}(0, I)$) into latent code (\mathbf{z}), getting:

$$\mathbf{z}_t = \sqrt{\bar{\alpha}_t} \mathbf{z} + \sqrt{1 - \bar{\alpha}_t} \epsilon, \quad (1)$$

where $\bar{\alpha}_t$ denotes a noise scheduler with timestep t . For the inverse process, it trains a denoising model (f_θ) with the objective:

$$\mathbb{E}_{\mathbf{z} \sim p(\mathbf{z}), \epsilon \sim \mathcal{N}(0, I), t} \left[\|\mathbf{y} - f_\theta(\mathbf{z}_t, \mathbf{c}, t)\|^2 \right], \quad (2)$$

where \mathbf{c} represents the condition and target \mathbf{y} can be noise ϵ , denoising input \mathbf{z} or v -prediction ($\mathbf{v} = \sqrt{\bar{\alpha}_t} \epsilon - \sqrt{1 - \bar{\alpha}_t} \mathbf{z}$) in (Salimans and Ho 2022). In this paper, we adopt the v -prediction as the supervision.

Zero terminal-SNR Noise Schedule. Previous studies proposed zero terminal SNR (Lin et al. 2024) to handle the signal-to-noise ratio (SNR) difference between the testing and training phase, which hinders the generation quality. At training, due to the residual signal left by the noise scheduler, the SNR is still not zero at the terminal timestep T . However, the sampler lacks realistic data when sampling from random gaussian noise during the test, resulting in a zero SNR. This train-test discrepancy is unreasonable and an obstacle to generating high-quality videos. Therefore, following the (Lin et al. 2024; Gupta et al. 2023; Girdhar et al. 2023), we scale up the noise schedule and set $\bar{\alpha}_T = 0$ to fix this problem.

Model Architecture

Fig. 3 illustrates the overall architecture of FancyVideo. The model is structured as a pseudo-3D UNet, which integrates frozen spatial blocks, sourced from a text-to-image model, along with Cross-frame Textual Guidance Modules (CTGM) and temporal attention blocks. The model takes three features as input: noisy latent $\mathcal{Z}_n \in \mathbb{R}^{f \times h \times w \times c}$, where h and w indicate the height and width of the latent, f signifies the number of frames, and c denotes the channels of the latent; mask indicator $\mathcal{M} \in \mathbb{R}^{f \times h \times w \times 1}$, with elements set to 1 for the first frame and 0 for all other frames; image indicator $\mathcal{I} \in \mathbb{R}^{f \times h \times w \times c}$, with initial image as the first frame and 0 for all other frames. The denoising input \mathcal{Z} is formed by concatenating \mathcal{Z}_n , \mathcal{M} and \mathcal{I} along the channel dimension, represented as $\mathcal{Z} = [\mathcal{Z}_n; \mathcal{M}; \mathcal{I}] \in \mathbb{R}^{f \times h \times w \times (2c+1)}$. Within each spatial block, CTGM is employed to capture the intricate dynamics described in the text prompts. Afterward, we apply temporal attention blocks to enhance the temporal relationships across various patches.

Cross-frame Textual Guidance Module

CTGM advances the existing text control method through three sub-modules: Temporal Information Injector (TII), Temporal Affinity Refiner (TAR), and Temporal Feature Booster (TFB) as depicted in Fig. (III). Before engaging in cross-attention, TII initially extracts temporal latent feature \mathcal{Z}_t and then incorporates temporal information into text embedding \mathcal{T}_{rep} based on \mathcal{Z}_t , obtaining cross-frame textual condition \mathcal{T}_z . Subsequently, TAR refines the affinity between \mathcal{Z}_t and \mathcal{T}_z along the time axis, enhancing the temporal coherence of textual guidance. Lastly, TFB further enhances the temporal continuity of the feature. The computation process of the CTGM can be formalized as:

$$\mathcal{Z}_t, \mathcal{T}_z = \text{TII}(\mathcal{Z}, \mathcal{T}_{rep}), \quad (3)$$

$$\mathcal{Z}'_{ref} = \text{TFB}\left(\text{Softmax}\left(\frac{\text{TAR}(W_q \mathcal{Z}_t, W_k \mathcal{T}_z)}{\sqrt{d_k}} W_v(\mathcal{T}_z)\right)\right), \quad (4)$$

where W_q , W_k , and W_v represent the linear layers for query, key, and value in original cross-attention, respectively. The hyper-parameter d_k is acquired from the query dimensions. $\text{TII}(\cdot, \cdot)$, $\text{TAR}(\cdot)$, $\text{TFB}(\cdot)$ denotes the TII, TAR and TFB. In the end, we get refined noisy latent feature \mathcal{Z}'_{ref} . A detailed description of these three modules is provided as follows.

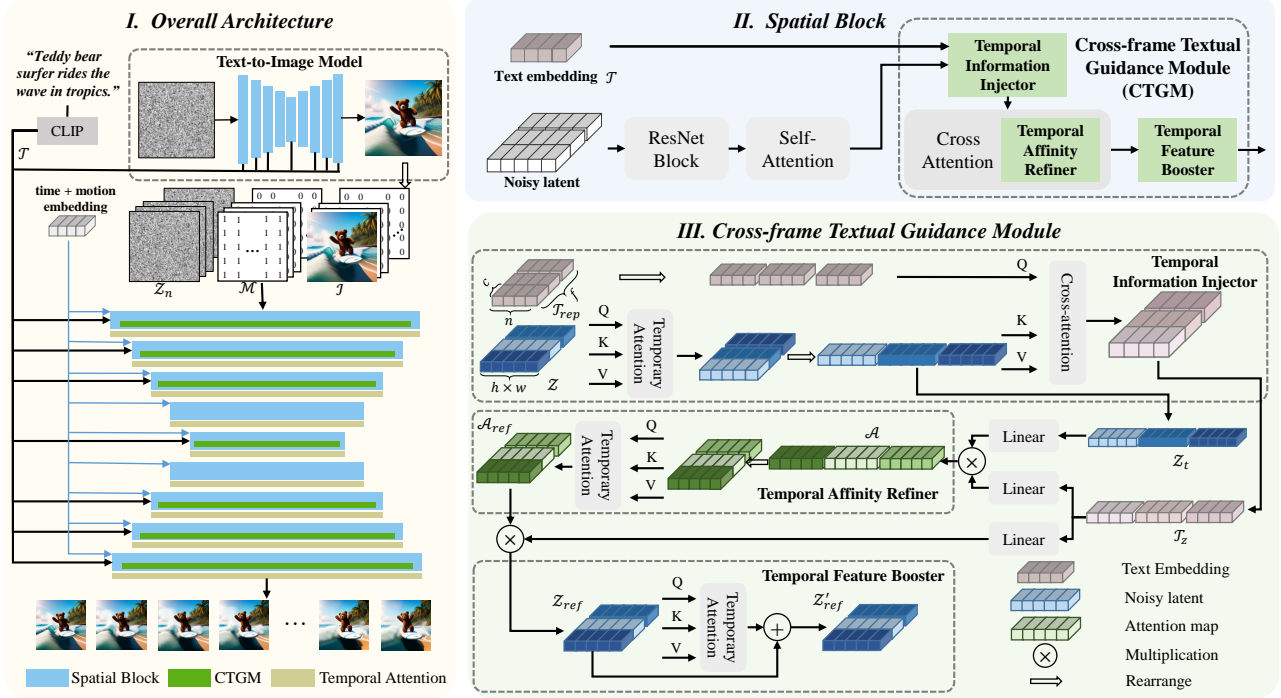


Figure 3: **The overall architecture of our method.** FancyVideo is a T+I2V model that concatenates noise latent, mask indicator, and image indicator as input. We insert our Cross-frame Textual Guidance Module (CTGM) into each spatial block. CTGM consists of three components: Temporal Information Injector, Temporal Affinity Refiner, and Temporal Feature Booster. These components are inserted at the beginning, middle, and end of cross-attention, respectively.

Temporal Information Injector. In previous work (Guo et al. 2023b; Girdhar et al. 2023), the text embedding \mathcal{T}_{rep} is repeated equally f times, resulting in $\mathcal{T}_{rep} \in \mathbb{R}^{f \times n \times c}$, n denoting the length of the embedding vector. We inject temporal information into the embedding before performing spatial cross-attention, thereby enabling distinct focal points on the text within different frames. In Temporal Information Injector (TII), we initially reshape the noisy latent \mathcal{Z} from $\mathbb{R}^{f \times h \times w \times c}$ to $\mathbb{R}^{(hw) \times f \times c}$ and apply temporal self-attention to acquire \mathcal{Z}_t . Then, we conduct spatial cross-attention, using the repeated text embedding \mathcal{T}_{rep} as queries and the noisy latent $\mathcal{Z}_t \in \mathbb{R}^{f \times (hw) \times c}$ as both keys and values, resulting in the text embedding \mathcal{T}_z with frame-specific temporal information. The formalization of the TII module can be expressed as follows:

$$\begin{aligned} \mathcal{Z}_t, \mathcal{T}_z &= \text{TII}(\mathcal{Z}, \mathcal{T}_{rep}) \\ &= \text{SelfAttn}_t(\mathcal{Z}), \\ &\quad \text{CrossAttn}_s(\text{SelfAttn}_t(\mathcal{Z}), \mathcal{T}_{rep}) \end{aligned} \quad (5)$$

where SelfAttn_t denotes temporal self-attention and CrossAttn_s denotes spatial cross-attention. Through TII, we obtain the noisy latent \mathcal{Z}_t with temporal information and the latent-aligned text embedding \mathcal{T}_z .

Temporal Affinity Refiner. To dynamically allocate attention to text embedding across different frames, we design the Temporal Affinity Refiner (TAR) to refine the attention map of spatial cross-attention. In spatial cross-attention, the noisy latent serves as the query, while the text embed-

ding serves as both the key and value. The attention map $\mathcal{A} \in \mathbb{R}^{f \times (hw) \times n}$, compute as $\mathcal{A} = (W_q \mathcal{Z}_t)(W_k \mathcal{T}_z)^T / \sqrt{d_k}$, reflects the affinity between the text and patches. Then, TAR applies temporal self-attention to the attention map $\mathcal{A} \in \mathbb{R}^{(hw) \times f \times n}$, obtaining the refined attention map \mathcal{A}_{ref} , which can be represented as:

$$\mathcal{A}_{ref} = \text{TAR}(\mathcal{A}) = \text{SelfAttn}_t(\mathcal{A}) \quad (6)$$

With the TAR, \mathcal{A}_{ref} establishes a more logical temporal connection in the affinity matrix. It can perform more dynamic action while ensuring no additional video distortion occurs. Finally, the cross-attention process is completed with the refined attention map as $\mathcal{Z}_{ref} = \text{Softmax}(\mathcal{A}_{ref})(W_v \mathcal{T}_z)$.

Temporal Feature Booster. To further boost the temporal consistency of the feature, we process the \mathcal{Z}_{ref} through the Temporal Feature Booster (TFB). This allows us to establish closer temporal connections. Specifically, TFB includes a simple yet effective temporal self-attention layer to refine the noisy latent feature along the time dimension, represented as:

$$\mathcal{Z}'_{ref} = \text{TFB}(\mathcal{Z}_{ref}) = \text{SelfAttn}_t(\mathcal{Z}_{ref}) + \mathcal{Z}_{ref} \quad (7)$$

Experiments

In the quantitative experiments, FancyVideo utilizes the T2I base model to generate images as the first frame. In the qualitative experiments, for aesthetic purposes and to remove watermarks, an external model is used to generate a beautiful first frame. Experimental setup about training data, settings, and hardware is provided in the supplementary material.

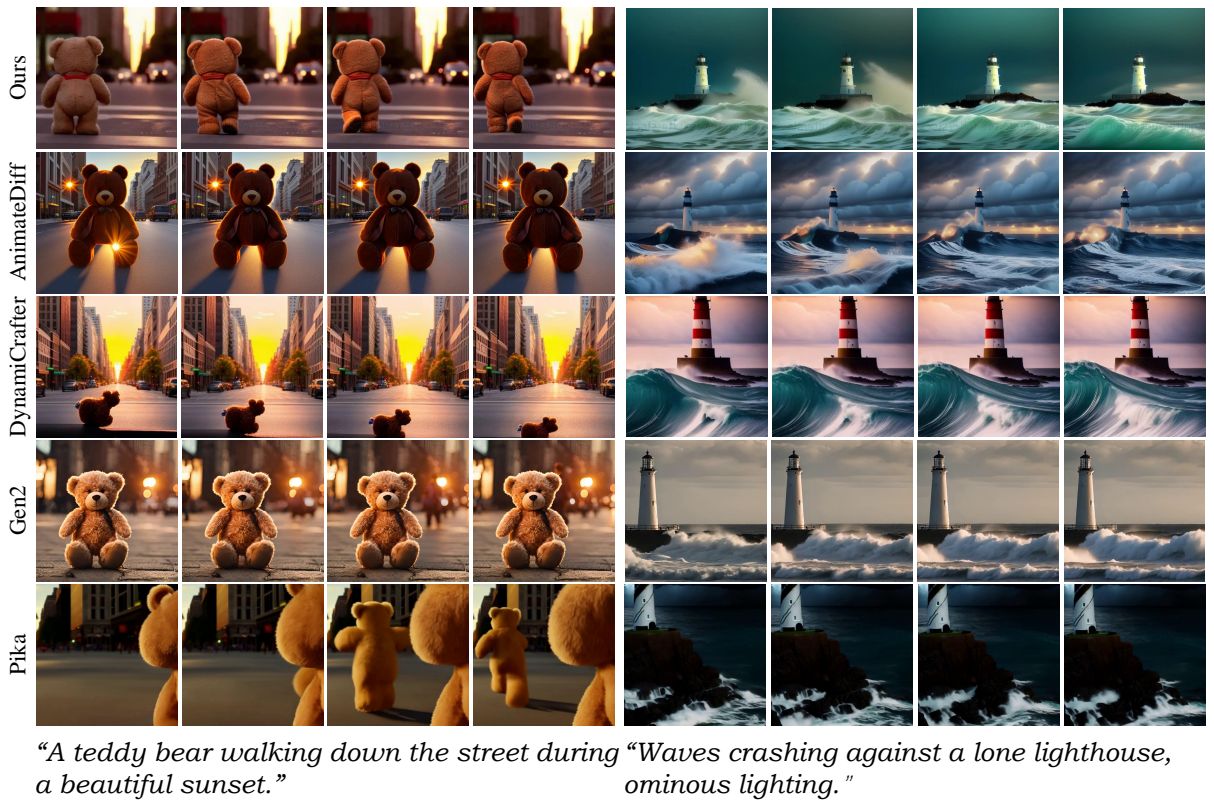
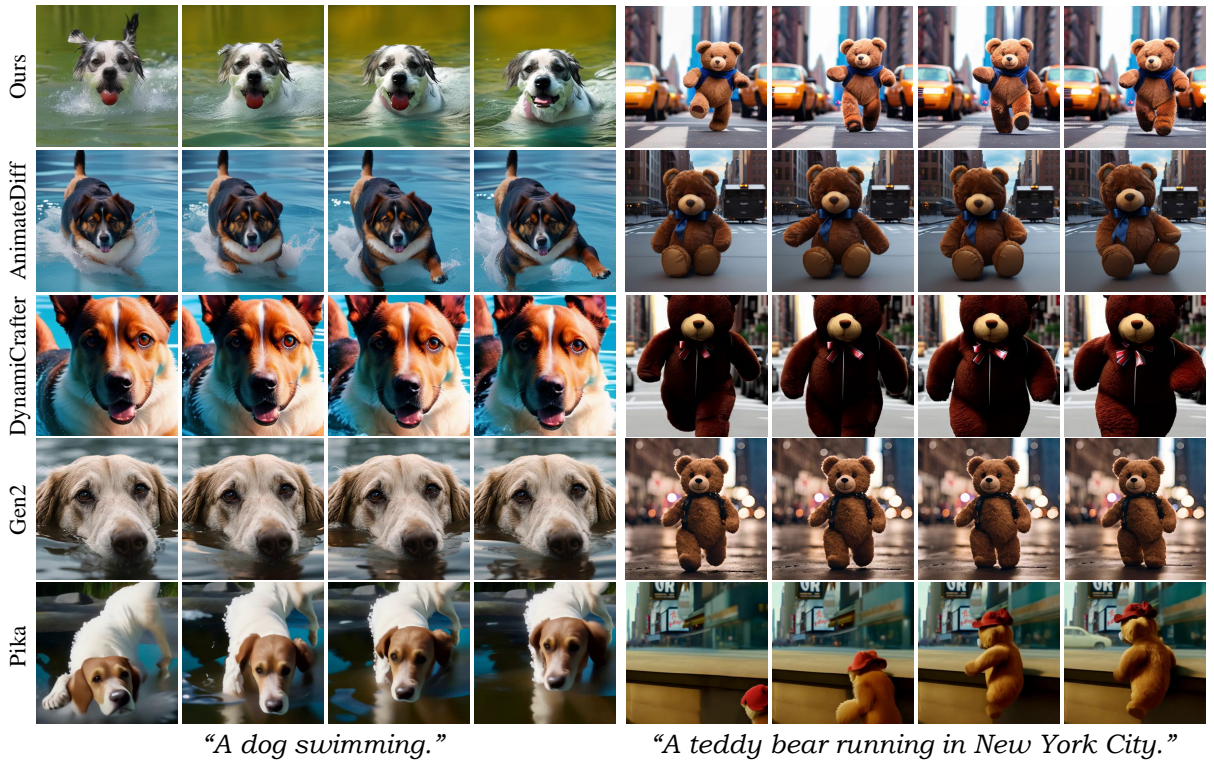


Figure 4: **Qualitative analysis.** We compare the video generation results from AnimateDiff (Guo et al. 2023b), DynamiCrafter (Xing et al. 2023), Pika (PikaLabs 2024), Gen-2 (Runway 2024), and our FancyVideo.

Table 1: **Quantitative evaluation on the EvalCrafter.** The best and second performing metrics are highlighted in **bold** and underline. Comprehensive denotes the composite metrics for these dimensions.

Dimensions Metrics		Pika(2024)	Gen2(2024)	Show-1(2023b)	Model-Scope(2023a)	Dynami-Crafter(2023)	Animate-Diff(2023b)	FancyVideo
Video Quality	VQAA(↑)	59.09	59.44	23.19	40.06	74.56	65.94	85.78
	VQAT(↑)	64.96	76.51	44.24	32.93	59.48	52.02	74.56
	IS(↑)	14.81	14.53	17.65	17.64	18.37	16.54	17.38
	Comprehensive(↑)	138.86	150.48	85.08	90.63	<u>152.41</u>	134.50	177.72
Text-Video Alignment	CLIP-Socre(↑)	20.46	20.53	20.66	20.36	20.80	19.70	20.85
	BLIP-BLEU(↑)	21.14	22.24	23.24	22.54	20.93	20.67	21.33
	SD-Score(↑)	68.57	68.58	68.42	67.93	67.87	66.13	68.14
	Detection-Score(↑)	58.99	64.05	58.63	50.01	64.04	51.19	66.66
	Color-Score(↑)	34.35	37.56	48.55	38.72	45.65	42.39	51.09
	Count-Score(↑)	51.46	53.31	44.31	44.18	53.53	22.40	59.19
	OCR Score(↓)	84.31	75.00	58.97	71.32	60.29	45.21	64.85
	Celebrity ID Score(↓)	45.31	41.25	37.93	44.56	26.35	42.26	25.76
Comprehensive(↑)	325.35	350.02	366.91	327.86	<u>386.18</u>	335.01	396.65	
Motion Quality	Action Score(↑)	71.81	62.53	81.56	72.12	72.22	61.94	72.99
	Motion AC-Score(→)	44	44	50	42	46	32	52
	Flow-Score(→)	0.50	0.70	2.07	6.99	0.96	2.403	1.7413
	Comprehensive(↑)	71.81	62.53	81.56	72.12	72.22	61.94	<u>72.99</u>
Temporal Consistency	CLIP-Temp(↑)	99.97	99.94	99.77	99.74	99.75	99.85	99.84
	Warping Error(↓)	0.0006	0.0008	0.0067	0.0162	0.0054	0.0177	0.0051
	Face Consistency(↑)	99.62	99.06	99.32	98.94	99.34	99.63	99.31
	Comprehensive(↑)	199.59	199.00	199.09	198.68	199.09	<u>199.48</u>	199.15

Qualitative Evaluation

We choose AnimateDiff (Guo et al. 2023b), DynamiCrafter (Xing et al. 2023), and two commercialized products, Pika (PikaLabs 2024) and Gen2 (Runway 2024), for a composite qualitative analysis. It is worth noting that in the quantitative experiments, the first frame of FancyVideo is generated by SDXL to achieve a more aesthetically pleasing result and to minimize the appearance of watermark (although subsequent frames may still exhibit it).

As shown in Fig. 4, our approach exhibits superior performance, outperforming previous methods regarding temporal consistency and motion richness. In contrast, AnimateDiff, DynamiCrafter, and Gen2 generate videos with less motion. Pika struggles to produce object-consistent and high-quality video frames. Remarkably, our method can accurately understand the motion instructions in the text prompt (e.g., "A teddy bear walking ... beautiful sunset." and "A teddy bear running ... City." case). More videos and applications (e.g., Personalized Video Generation and Video Extending) are provided in our supplementary material.

Quantitative Evaluation

For a comprehensive comparison with the SOTA methods, we adopt three popular benchmarks (e.g., EvalCrafter (Liu et al. 2023), UCF-101 (Soomro, Zamir, and Shah 2012), and MSR-VTT (Xu et al. 2016)) and human evaluation to evaluate the quality of video generation. Among them, EvalCrafter is a relatively comprehensive benchmark for video generation currently. UCF-101 and MSR-VTT are benchmarks commonly used in previous methods (Girdhar

et al. 2023; Zhang et al. 2023b). Meanwhile, human evaluation can compensate for the inaccuracies in existing text-conditioned video generation evaluation systems.

EvalCrafter Benchmark. EvalCrafter (Liu et al. 2023) quantitatively evaluates the quality of text-to-video generation from four aspects (including Video Quality, Text-video Alignment, Motion Quality, and Temporal Consistency). Each dimension contains multiple subcategories of indicators shown in the Table. 1. As discussed in community (Liu and Cun 2024), the authors acknowledge that the original manner of calculating the comprehensive metric was inappropriate. For a more intuitive comparison, we introduce a comprehensive metric for every aspect by considering each sub-indicators numerical scale and positive-negative attributes. Detailed information about the comprehensive metric can be available in supplementary material.

In detail, we compare the performance of the previous video generation SOTA methods (e.g., Pika (PikaLabs 2024), Gen2 (Runway 2024), Show-1 (Zhang et al. 2023b), ModelScope (Wang et al. 2023a), DynamiCrafter (Xing et al. 2023), and AnimateDiff (Guo et al. 2023b)) and exhibit in Table. 1. Our method demonstrates outstanding performance beyond existing methods at the Video Quality and Text-video Alignment aspect. Although Show-1 has the best Motion Quality (81.56), its Video Quality is poor (only 85.08). That indicates that it cannot generate high-quality videos with reasonable motion. However, our method has the second highest Motion Quality (72.99) and the best Video Quality (177.72), achieving the trade-off between

Table 2: **Quantitative evaluation on the UCF-101 (Soomro, Zamir, and Shah 2012) and MSR-VTT (Xu et al. 2016)**. The best and second performing metrics are highlighted in **bold** and underline respectively.

Method	Data	UCF-101			MSR-VTT	
		FVD(↓)	IS(↑)	FID(↓)	FVD(↓)	CLIPSIM (↑)
Emu Video (2023)	34M	606.20	<u>42.70</u>	-	-	-
AnimateDiff (2023b)	10M	584.85	37.01	61.24	628.57	0.2881
DynamiCrafter (2023)	10M	404.50	41.97	32.35	219.31	0.2659
Show-1 (2023b)	10M	394.46	35.42	-	538.00	0.3072
ModelScope (2023a)	10M	410.00	-	-	550.00	0.2939
FancyVideo	10M	412.64	43.66	<u>47.01</u>	<u>333.52</u>	0.3076

Table 3: **Ablation studies** on the core component of FancyVideo.

TAR	TFB	TII	Video Quality	Text-Video Alignment	Motion Quality	Temporal Consistency
			163.15	361.92	66.99	198.83
✓			172.44	379.40	71.24	199.08
	✓		167.64	369.40	68.46	198.78
		✓	165.15	364.40	65.59	199.01
✓	✓		175.82	390.24	71.84	199.02
✓	✓	✓	177.72	396.65	72.99	199.15

quality and motion. The above results indicate the superiority of FancyVideo and its ability to generate temporal-consistent and motion-accurate video.

UCF-101 & MSR-VTT. Following the prior work (Zhang et al. 2023b), we evaluate the zero-shot generation performance on UCF-101 (Soomro, Zamir, and Shah 2012) and MSR-VTT (Xu et al. 2016) as shown in Table. 2. We use Fréchet Video Distance (FVD) (Unterthiner et al. 2019), Inception Score (IS) (Wu et al. 2021), Fréchet Inception Distance (FID) (Heusel et al. 2017), and CLIP similarity (CLIPSIM) as evaluation metrics and compared some current SOTA methods. FancyVideo achieves competitive results, particularly excelling in IS and CLIPSIM with scores of 43.66 and 0.3076, respectively. Besides, previous studies (Ho et al. 2022; Girdhar et al. 2023; Wu et al. 2023b) have pointed out that these metrics do not accurately reflect human perception and are affected by the gap between the distribution of training and test data and the image’s low-level detail.

Human Evaluation. Inspired by EvalCrafter (Liu et al. 2023), we introduce a multi-candidate ranking protocol with four aspects: video quality, text-video alignment, motion quality, and temporal consistency. In this protocol, participants rank the results of multiple candidate models for each aspect. Each candidate model receives a score based on its ranking. For instance, if there are N candidate models ranked by video quality, the first model gets $N - 1$ points, the second gets $N - 2$ points, and so on, with the last model receiving 0 points. Adhering to this protocol, we selected 108 samples from the EvalCrafter validation set and gathered judgments from 100 individuals. As depicted in Fig. 5, our

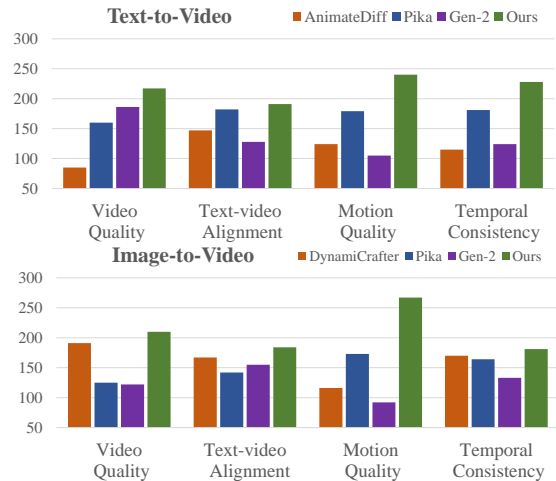


Figure 5: **Human Evaluation Comparison.** FancyVideo stands out significantly compared to other text-to-video and image-to-video generators in terms of Motion Quality and Temporal Consistency.

method significantly outperforms text-to-video conversion methods, including AnimateDiff (Guo et al. 2023b), Pika (PikaLabs 2024), and Gen2 (Runway 2024), across all four aspects. FancyVideo demonstrates exceptional motion quality while preserving superior text-video consistency. Additionally, we conducted a similar comparison of four image-to-video methods, including DynamiCrafter (Xing et al. 2023), Pika, and Gen2, as shown in Fig. 5.

Ablation Studies

In this section, we conduct the experiment and exhibit the visual comparison on the EvalCrafter (Liu et al. 2023) to explore the effect of critical design in CTGM. Specifically, the ablation component contains the three core modules (TII, TAR, and TFB). As shown in Table. 3, TAR can effectively improve the performance on both metrics, showing that temporal refined attention map operations are beneficial for video generation. Continued insertion of TFB and TII further improves the generator’s performance, due to the refined latent features and frame-level personalized text condition. Meanwhile, the qualitative analysis is included in the appendix.

Conclusion

In this work, we present a novel video-generation method named FancyVideo, which optimizes common text control mechanisms (e.g., spatial cross-attention) from the cross-frame textual guidance. It improves cross-attention with a well-designed Cross-frame Textual Guidance Module (CTGM), implementing the temporal-specific textual condition guidance for video generation. A comprehensive qualitative and quantitative analysis shows it can produce more dynamic and consistent videos. This characteristic becomes more noticeable as the number of frames increases. Our method achieves state-of-the-art results on the EvalCrafter benchmark and human evaluations.

References

- Bain, M.; Nagrani, A.; Varol, G.; and Zisserman, A. 2021. Frozen in time: A joint video and image encoder for end-to-end retrieval. In *Proceedings of the IEEE/CVF International Conference on Computer Vision*, 1728–1738.
- Blattmann, A.; Dockhorn, T.; Kulal, S.; Mendelevitch, D.; Kilian, M.; Lorenz, D.; Levi, Y.; English, Z.; Voleti, V.; Letts, A.; et al. 2023a. Stable video diffusion: Scaling latent video diffusion models to large datasets. *arXiv preprint arXiv:2311.15127*.
- Blattmann, A.; Rombach, R.; Ling, H.; Dockhorn, T.; Kim, S. W.; Fidler, S.; and Kreis, K. 2023b. Align your latents: High-resolution video synthesis with latent diffusion models. In *Proceedings of the IEEE/CVF Conference on Computer Vision and Pattern Recognition*, 22563–22575.
- Chen, X.; Wang, Y.; Zhang, L.; Zhuang, S.; Ma, X.; Yu, J.; Wang, Y.; Lin, D.; Qiao, Y.; and Liu, Z. 2023. Seine: Short-to-long video diffusion model for generative transition and prediction. In *The Twelfth International Conference on Learning Representations*.
- Cheng, J.; Xie, P.; Xia, X.; Li, J.; Wu, J.; Ren, Y.; Li, H.; Xiao, X.; Zheng, M.; and Fu, L. 2024. ResAdapter: Domain Consistent Resolution Adapter for Diffusion Models. *arXiv preprint arXiv:2403.02084*.
- Civitai. 2024. Civitai Community Discord Server. <https://civitai.com/>.
- De Luigi, L.; Cardace, A.; Spezialetti, R.; Ramirez, P. Z.; Salti, S.; and Di Stefano, L. 2023. Deep learning on implicit neural representations of shapes. *arXiv preprint arXiv:2302.05438*.
- Ge, S.; Nah, S.; Liu, G.; Poon, T.; Tao, A.; Catanzaro, B.; Jacobs, D.; Huang, J.-B.; Liu, M.-Y.; and Balaji, Y. 2023. Preserve your own correlation: A noise prior for video diffusion models. In *Proceedings of the IEEE/CVF International Conference on Computer Vision*, 22930–22941.
- Girdhar, R.; Singh, M.; Brown, A.; Duval, Q.; Azadi, S.; Rambhatla, S. S.; Shah, A.; Yin, X.; Parikh, D.; and Misra, I. 2023. Emu video: Factorizing text-to-video generation by explicit image conditioning. *arXiv preprint arXiv:2311.10709*.
- Guo, X.; Zheng, M.; Hou, L.; Gao, Y.; Deng, Y.; Ma, C.; Hu, W.; Zha, Z.; Huang, H.; Wan, P.; et al. 2023a. I2V-Adapter: A General Image-to-Video Adapter for Video Diffusion Models. *arXiv preprint arXiv:2312.16693*.
- Guo, Y.; Yang, C.; Rao, A.; Wang, Y.; Qiao, Y.; Lin, D.; and Dai, B. 2023b. Animatediff: Animate your personalized text-to-image diffusion models without specific tuning. *arXiv preprint arXiv:2307.04725*.
- Gupta, A.; Yu, L.; Sohn, K.; Gu, X.; Hahn, M.; Fei-Fei, L.; Essa, I.; Jiang, L.; and Lezama, J. 2023. Photorealistic video generation with diffusion models. *arXiv preprint arXiv:2312.06662*.
- Gur, S.; Benaim, S.; and Wolf, L. 2020. Hierarchical patch vae-gan: Generating diverse videos from a single sample. *Advances in Neural Information Processing Systems*, 33: 16761–16772.
- Heusel, M.; Ramsauer, H.; Unterthiner, T.; Nessler, B.; and Hochreiter, S. 2017. Gans trained by a two time-scale update rule converge to a local nash equilibrium. *Advances in neural information processing systems*, 30.
- Ho, J.; Chan, W.; Saharia, C.; Whang, J.; Gao, R.; Gritsenko, A.; Kingma, D. P.; Poole, B.; Norouzi, M.; Fleet, D. J.; et al. 2022. Imagen video: High definition video generation with diffusion models. *arXiv preprint arXiv:2210.02303*.
- Ho, J.; Jain, A.; and Abbeel, P. 2020. Denoising diffusion probabilistic models. *Advances in neural information processing systems*, 33: 6840–6851.
- Ho, J.; and Salimans, T. 2022. Classifier-free diffusion guidance. *arXiv preprint arXiv:2207.12598*.
- Jiang, Y.; Wu, T.; Yang, S.; Si, C.; Lin, D.; Qiao, Y.; Loy, C. C.; and Liu, Z. 2023. VideoBooth: Diffusion-based Video Generation with Image Prompts. *arXiv preprint arXiv:2312.00777*.
- Kingma, D. P.; and Welling, M. 2013. Auto-encoding variational bayes. *arXiv preprint arXiv:1312.6114*.
- Lin, S.; Liu, B.; Li, J.; and Yang, X. 2024. Common diffusion noise schedules and sample steps are flawed. In *Proceedings of the IEEE/CVF Winter Conference on Applications of Computer Vision*, 5404–5411.
- Liu, Y.; and Cun, X. 2024. evalcrafter github project. <https://github.com/evalcrafter/evalcrafter>.
- Liu, Y.; Cun, X.; Liu, X.; Wang, X.; Zhang, Y.; Chen, H.; Liu, Y.; Zeng, T.; Chan, R.; and Shan, Y. 2023. Evalcrafter: Benchmarking and evaluating large video generation models. *arXiv preprint arXiv:2310.11440*.
- Luo, Z.; Chen, D.; Zhang, Y.; Huang, Y.; Wang, L.; Shen, Y.; Zhao, D.; Zhou, J.; and Tan, T. 2023. Decomposed diffusion models for high-quality video generation. *arXiv preprint arXiv:2303.08320*.
- Menapace, W.; Siarohin, A.; Skorokhodov, I.; Deyneka, E.; Chen, T.-S.; Kag, A.; Fang, Y.; Stoliar, A.; Ricci, E.; Ren, J.; et al. 2024. Snap Video: Scaled Spatiotemporal Transformers for Text-to-Video Synthesis. *arXiv preprint arXiv:2402.14797*.
- Munoz, A.; Zolfaghari, M.; Argus, M.; and Brox, T. 2021. Temporal shift GAN for large scale video generation. In *Proceedings of the IEEE/CVF Winter Conference on Applications of Computer Vision*, 3179–3188.
- PikaLabs. 2024. Pika Lab Discord Server. <https://www.pika.art/>.
- Ramesh, A.; Pavlov, M.; Goh, G.; Gray, S.; Voss, C.; Radford, A.; Chen, M.; and Sutskever, I. 2021. Zero-shot text-to-image generation. In *International conference on machine learning*, 8821–8831. Pmlr.
- Razavi, A.; Van den Oord, A.; and Vinyals, O. 2019. Generating diverse high-fidelity images with vq-vae-2. *Advances in neural information processing systems*, 32.
- Ren, W.; Yang, H.; Zhang, G.; Wei, C.; Du, X.; Huang, S.; and Chen, W. 2024. ConsistI2V: Enhancing Visual Consistency for Image-to-Video Generation. *arXiv preprint arXiv:2402.04324*.

- Rombach, R.; Blattmann, A.; Lorenz, D.; Esser, P.; and Ommer, B. 2022. High-resolution image synthesis with latent diffusion models. In *Proceedings of the IEEE/CVF conference on computer vision and pattern recognition*, 10684–10695.
- Ruiz, N.; Li, Y.; Jampani, V.; Pritch, Y.; Rubinstein, M.; and Aberman, K. 2023. Dreambooth: Fine tuning text-to-image diffusion models for subject-driven generation. In *Proceedings of the IEEE/CVF Conference on Computer Vision and Pattern Recognition*, 22500–22510.
- Runway. 2024. Gen2 Discord Server. <https://research.runwayml.com/gen2/>.
- Saito, M.; Saito, S.; Koyama, M.; and Kobayashi, S. 2020. Train sparsely, generate densely: Memory-efficient unsupervised training of high-resolution temporal gan. *International Journal of Computer Vision*, 128(10): 2586–2606.
- Salimans, T.; and Ho, J. 2022. Progressive distillation for fast sampling of diffusion models. *arXiv preprint arXiv:2202.00512*.
- Sohl-Dickstein, J.; Weiss, E.; Maheswaranathan, N.; and Ganguli, S. 2015. Deep unsupervised learning using nonequilibrium thermodynamics. In *International conference on machine learning*, 2256–2265. PMLR.
- Song, J.; Meng, C.; and Ermon, S. 2020. Denoising diffusion implicit models. *arXiv preprint arXiv:2010.02502*.
- Soomro, K.; Zamir, A. R.; and Shah, M. 2012. A dataset of 101 human action classes from videos in the wild. *Center for Research in Computer Vision*, 2(11): 1–7.
- Unterthiner, T.; van Steenkiste, S.; Kurach, K.; Marinier, R.; Michalski, M.; and Gelly, S. 2019. FVD: A new metric for video generation.
- Wang, J.; Yuan, H.; Chen, D.; Zhang, Y.; Wang, X.; and Zhang, S. 2023a. Modelscope text-to-video technical report. *arXiv preprint arXiv:2308.06571*.
- Wang, T.-H.; Cheng, Y.-C.; Lin, C. H.; Chen, H.-T.; and Sun, M. 2019. Point-to-point video generation. In *Proceedings of the IEEE/CVF international conference on computer vision*, 10491–10500.
- Wang, W.; Liu, J.; Lin, Z.; Yan, J.; Chen, S.; Low, C.; Hoang, T.; Wu, J.; Liew, J. H.; Yan, H.; et al. 2024. MagicVideo-V2: Multi-Stage High-Aesthetic Video Generation. *arXiv preprint arXiv:2401.04468*.
- Wang, Y.; Bilinski, P.; Bremond, F.; and Dantcheva, A. 2020. Imaginator: Conditional spatio-temporal gan for video generation. In *Proceedings of the IEEE/CVF Winter Conference on Applications of Computer Vision*, 1160–1169.
- Wang, Y.; Chen, X.; Ma, X.; Zhou, S.; Huang, Z.; Wang, Y.; Yang, C.; He, Y.; Yu, J.; Yang, P.; et al. 2023b. Lavie: High-quality video generation with cascaded latent diffusion models. *arXiv preprint arXiv:2309.15103*.
- Wu, C.; Huang, L.; Zhang, Q.; Li, B.; Ji, L.; Yang, F.; Sapiro, G.; and Duan, N. 2021. Godiva: Generating open-domain videos from natural descriptions. *arXiv preprint arXiv:2104.14806*.
- Wu, J. Z.; Ge, Y.; Wang, X.; Lei, S. W.; Gu, Y.; Shi, Y.; Hsu, W.; Shan, Y.; Qie, X.; and Shou, M. Z. 2023a. Tune-a-video: One-shot tuning of image diffusion models for text-to-video generation. In *Proceedings of the IEEE/CVF International Conference on Computer Vision*, 7623–7633.
- Wu, T.; Si, C.; Jiang, Y.; Huang, Z.; and Liu, Z. 2023b. Freeinit: Bridging initialization gap in video diffusion models. *arXiv preprint arXiv:2312.07537*.
- Xing, J.; Xia, M.; Liu, Y.; Zhang, Y.; He, Y.; Liu, H.; Chen, H.; Cun, X.; Wang, X.; Shan, Y.; et al. 2024. Make-Your-Video: Customized Video Generation Using Textual and Structural Guidance. *IEEE Transactions on Visualization and Computer Graphics*.
- Xing, J.; Xia, M.; Zhang, Y.; Chen, H.; Wang, X.; Wong, T.-T.; and Shan, Y. 2023. Dynamicrafter: Animating open-domain images with video diffusion priors. *arXiv preprint arXiv:2310.12190*.
- Xu, J.; Mei, T.; Yao, T.; and Rui, Y. 2016. Msr-vtt: A large video description dataset for bridging video and language. In *Proceedings of the IEEE conference on computer vision and pattern recognition*, 5288–5296.
- Yan, W.; Zhang, Y.; Abbeel, P.; and Srinivas, A. 2021. Videogpt: Video generation using vq-vae and transformers. *arXiv preprint arXiv:2104.10157*.
- Yu, J.; Cun, X.; Qi, C.; Zhang, Y.; Wang, X.; Shan, Y.; and Zhang, J. 2023. AnimateZero: Video Diffusion Models are Zero-Shot Image Animators. *arXiv preprint arXiv:2312.03793*.
- Zeng, Y.; Wei, G.; Zheng, J.; Zou, J.; Wei, Y.; Zhang, Y.; and Li, H. 2023. Make pixels dance: High-dynamic video generation. *arXiv preprint arXiv:2311.10982*.
- Zhang, C.; Zhang, C.; Zhang, M.; and Kweon, I. S. 2023a. Text-to-image diffusion model in generative ai: A survey. *arXiv preprint arXiv:2303.07909*.
- Zhang, D. J.; Li, D.; Le, H.; Shou, M. Z.; Xiong, C.; and Sahoo, D. 2024. Moonshot: Towards controllable video generation and editing with multimodal conditions. *arXiv preprint arXiv:2401.01827*.
- Zhang, D. J.; Wu, J. Z.; Liu, J.-W.; Zhao, R.; Ran, L.; Gu, Y.; Gao, D.; and Shou, M. Z. 2023b. Show-1: Marrying pixel and latent diffusion models for text-to-video generation. *arXiv preprint arXiv:2309.15818*.
- Zhang, L.; Rao, A.; and Agrawala, M. 2023. Adding conditional control to text-to-image diffusion models. In *Proceedings of the IEEE/CVF International Conference on Computer Vision*, 3836–3847.
- Zhou, D.; Wang, W.; Yan, H.; Lv, W.; Zhu, Y.; and Feng, J. 2022. Magicvideo: Efficient video generation with latent diffusion models. *arXiv preprint arXiv:2211.11018*.
- Zhu, J.-Y.; Park, T.; Isola, P.; and Efros, A. A. 2017. Unpaired image-to-image translation using cycle-consistent adversarial networks. In *Proceedings of the IEEE international conference on computer vision*, 2223–2232.

Supplementary material

Overview. In this supplemental material, we provide the following items:

- (Sec. 1) Experimental setup.
- (Sec. 2) More details on evaluation metrics employed in UCF101, MSR-VTT, human evaluation and the EvalCrafter (Liu et al. 2023).
- (Sec. 3) More applications about Personalized Video Generation, high-resolution and multi-scale Video Generation, Video Predication and Video Backtracking, among others.
- (Sec. 4) More results on video generation, including videos with different frame rates.
- (Sec. 5) Prompts set for human evaluation.

Experimental Setup

Datasets. We utilize WebVid-10M (Bain et al. 2021) as the training data. The WebVid-10M dataset contains 10.7 million video-caption pairs, with most videos having a resolution of 336×596 . Since every clip in the WebVid-10M has a watermark, the generated video inevitably appears watermarked.

Implementation details. FancyVideo is trained on the WebVid-10M dataset. The video clips are initially sampled with a stride of 4, followed by resizing and center-cropping to a resolution of 256×256 . We utilize Stable-Diffusion v1.5 (Rombach et al. 2022) as the text-to-image (T2I) base model and train exclusively with the temporal attention block and our CTGM block. For the 16-frame training, we use a batch size of 512 and train for 12,000 iterations. For training with 32 frames, 48 frames, and 64 frames, we use batch sizes of 256, 256, and 128, respectively. The training process comprises 24,000 iterations for 32 frames, 48,000 iterations for 48 frames, and 96,000 iterations for 64 frames on 64 A100 GPUs with 80G memory. At inference, the sampling strategy for video generation is DDIM (Song, Meng, and Ermon 2020) with 50 steps. Also, we utilize the classifier-free guidance (Ho and Salimans 2022) with a 7.5 guidance scale. Similar to AnimateDiff (Guo et al. 2023b), we swap the base model with Realistic-Vision v5.1. The evaluations on EvalCrafter (Liu et al. 2023) and all the qualitative experiments are conducted at a resolution of 512. Regarding the evaluations on UCF-101 (Soomro, Zamir, and Shah 2012) and MSR-VTT (Xu et al. 2016), following (Zhang et al. 2023b), we conduct assessments on videos generated at a resolution of 256.

More Details on Evaluation Metrics

Details of evaluation on UCF101 To calculate the Fréchet Video Distance (FVD) (Unterthiner et al. 2019) and Inception Score (IS) (Blattmann et al. 2023b; Ren et al. 2024; Saito et al. 2020), we produce 2048 videos based on the class distribution of the UCF101 dataset. These videos are generated at a resolution of 256 pixels. Subsequently, we extract I3D embeddings from our videos. Next, we compute the FVD score by comparing the I3D embeddings of our videos with those of the UCF101 videos. For computing the

Inception Score (IS), the same set of generated videos was utilized to extract C3D embeddings.

Details of evaluation on MSR-VTT The MSR-VTT dataset is an open-domain video retrieval and captioning dataset with 10,000 videos, each having 20 captions. The standard splits include 6,513 training videos, 497 validation videos, and 2,990 test videos. For our experiments, we use the official test split and randomly select a text prompt for each video during evaluation. Using TorchMetrics, we compute our CLIPSIM (Wu et al. 2021) metrics with the CLIP-VIT-B/32 model. We calculate the CLIP similarity for all frames in the generated videos and report the averaged results.

Details of Human Evaluation We filter out 108 prompts from the 700 prompts in EvalCrafter for human evaluation. This subset of prompts contains more detailed descriptions. The prompt-108 we utilized is presented in .

About EvalCrafter As mentioned in , there are unreasonable aspects in how EvalCrafter calculates Video Quality, Text-Video Alignment, Motion Quality, and Temporal Consistency. Therefore, we propose our calculation scheme. Specifically, we remove some neutral sub-metrics and those with significant differences in scale, and based on whether each sub-metric is positive or negative, we obtain a comprehensive score. For Video Quality, it can be represented as follows:

$$Video_Quality = VQAA + VQAT + IS \quad (8)$$

As for Text-Video Alignment, it can be represented as:

$$\begin{aligned} Text_Video_Alignment = & CLIP_Score + SD_Score \\ & + BLIP_BLEU \\ & + Count_Score + Color_Score \\ & + Detection_Score \\ & + (100 - OCR_Score) \\ & + (100 - Celebrity_ID_Score) \end{aligned}$$

As for Motion Quality, we do not consider neutral metrics when calculating:

$$Motion_Quality = Action_Score \quad (9)$$

As for Temporal Consistency, we neglect the warping error, which has a scale that differs significantly from other metrics:

$$Temporal_Consistency = CLIP_Temp + Face_Consistency \quad (10)$$

$$\begin{aligned} Temporal_Consistency = & CLIP_Temp \\ & + Face_Consistency \end{aligned}$$

More Applications

Given the flexibility of our method in swapping T2I base models, we conduct experiments similar to prior work (Guo et al. 2023b), with different base models. Fig. 7 displays the

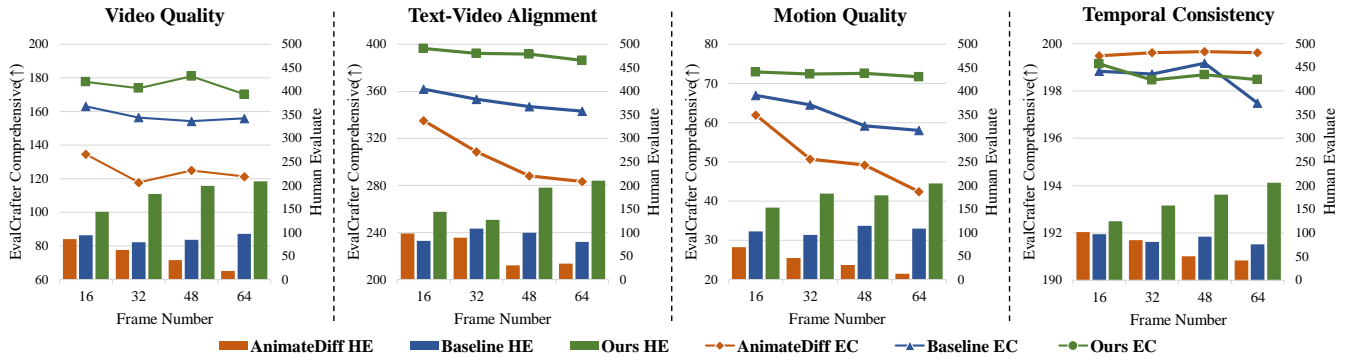


Figure 6: **Evaluation results of varying-frames video generation.** EC denotes the comprehensive metric on EvalCrafter(Liu et al. 2023) benchmark and HE indicates Human Evaluation.

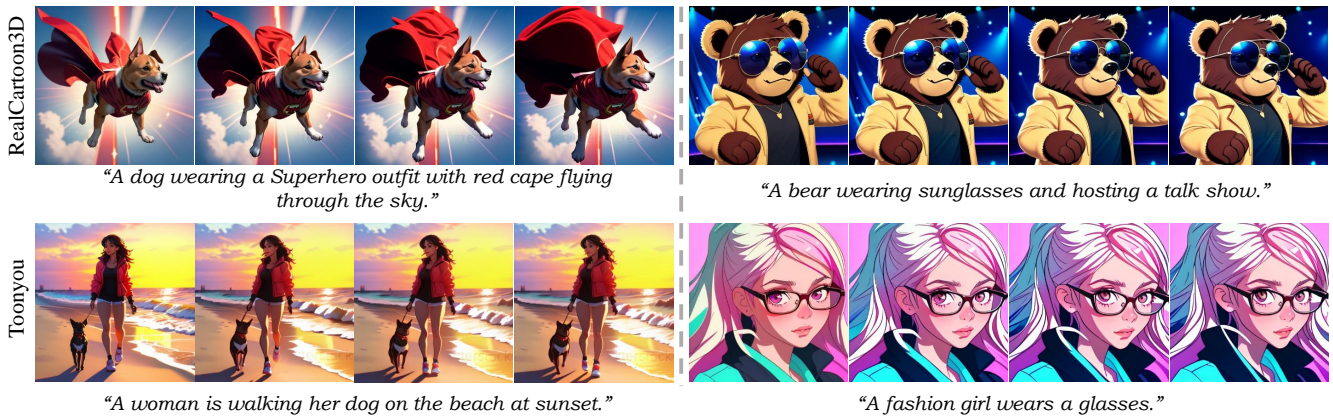


Figure 7: **Qualitative experiments.** We demonstrate the ability to generate personalized videos by using various T2I-based models.

results of our method using models downloaded from the Civitai(Civitai 2024) community.

Due to the specificity of our input, we investigate the potential of our model to perform additional functionalities by modifying the mask indicator and image indicator. This encompasses tasks such as Video Prediction and Video Extending, as depicted in Fig. 8 and Fig. 9.

Due to the flexibility of our framework, we can easily combine our method with text-to-image super-resolution modules (Cheng et al. 2024). We conduct experiments to achieve multi-scale and high-resolution video generations, as depicted in Fig. 12.

More Generation Results

We further showcase additional results of the FancyVideo generation, including videos with 16 frames, 32 frames, 48 frames, and 64 frames. As shown in Fig. 13, our method effectively maintains consistency while also addressing motion dynamics.

The qualitative analysis in Fig. 10 demonstrates the experimental results of training with and without CTGM. In the upper case, without CTGM, the text is not fully understood, causing the subject in the red box to be unnaturally still. In bottom case, there is a distortion in the red dashed

circle. With CTGM, our model generates more dynamic and undistorted videos.

A list of prompts for human evaluation

1. goldfish in glass
2. A peaceful cow grazing in a green field under the clear blue sky
3. A fluffy grey and white cat is lazily stretched out on a sunny window sill, enjoying a nap after a long day of lounging.
4. a horse
5. Two elephants are playing on the beach and enjoying a delicious beef stroganoff meal.
6. A slithering snake moves through the lush green grass
7. A cute and chubby giant panda is enjoying a bamboo meal in a lush forest. The panda is relaxed and content as it eats, and occasionally stops to scratch its ear with its paw.
8. Pikachu snowboarding
9. a dog wearing vr goggles on a boat



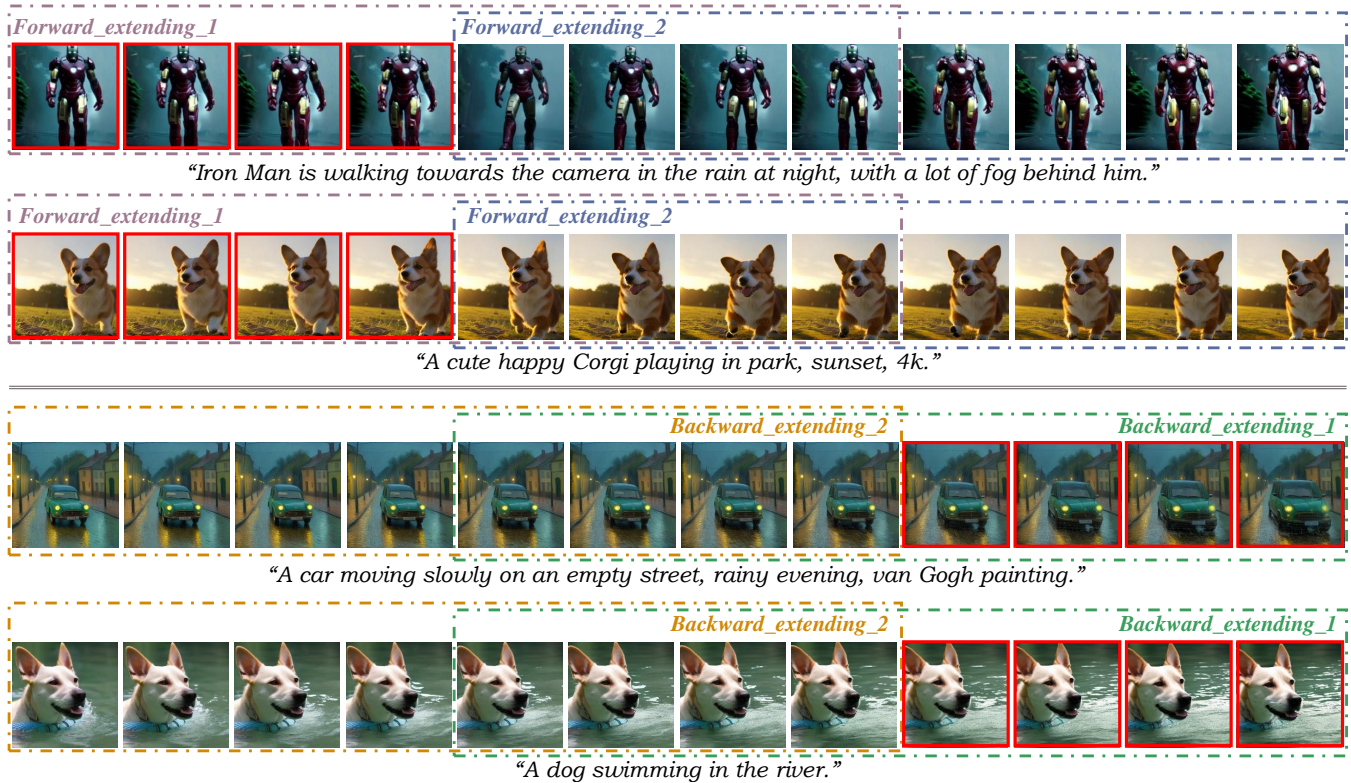
“A photo of a Corgi dog riding a bike in Times Square. It is wearing sunglasses and a beach hat.”



“Valkyrie riding flying horses through the clouds.”

Figure 8: **Qualitative experiments.** Under the FancyVideo framework, we train the **Video Interpolation** model. The red border indicates the first four frames of the original video, and we inserted three frames between every two original frames.

10. In an African savanna, a majestic lion is prancing behind a small timid rabbit. The rabbit tried to run away, but the lion catches up easily.
11. A photo of a Corgi dog riding a bike in Times Square. It is wearing sunglasses and a beach hat.
12. In the lush forest, a tiger is wandering around with a vigilant gaze while the birds chirp and monkeys play.
13. A family of four fluffy, blue penguins waddled along the icy shore.
14. Two white swans gracefully swam in the serene lake
15. A bear rummages through a dumpster, searching for food scraps.
16. light wind, feathers moving, she moves her gaze, 4k
17. fashion portrait shoot of a girl in colorful glasses, a breeze moves her hair
18. Two birds flew around a person, in the style of Sci-Fi
19. flying superman, hand moves forward
20. Batman turns his head from right to left
21. Iron Man is walking towards the camera in the rain at night, with a lot of fog behind him. Science fiction movie, close-up
22. Bruce Lee shout like a lion ,wild fighter
23. A woman is walking her dog on the beach at sunset.
24. Valkyrie riding flying horses through the clouds
25. A surfer paddles out into the ocean, scanning the waves for the perfect ride.
26. A man cruises through the city on a motorcycle, feeling the adrenaline rush
27. A musician strums his guitar, serenading the moonlit night
28. Leaves falling in autumn forest
29. Thunderstorm at night
30. A snow avalanche crashed down a mountain peak, causing destruction and mayhem
31. A thick fog covers a street, making it nearly impossible to see. Cars headlights pierce through the mist as they slowly make their way down the road.
32. The flowing water sparkled under the golden sunrise in a peaceful mountain river.
33. A warm golden sunset on the beach, with waves gently lapping the shore.
34. Mount Fuji
35. A beautiful leather handbag caught my eye in the store window. It had a classic shape and was a rich cognac color. The material was soft and supple. The golden text label on the front read 'Michael Kors'.
36. balloons flying in the air
37. a motorcycle race through the city streets at night
38. A silver metal train with blue and red stripes, speeding through a mountainous landscape.
39. hot ramen
40. Juicy and sweet mangoes lying in a woven basket
41. A delicious hamburger with juicy beef patty, crispy lettuce and melted cheese.
42. In Marvel movie style, supercute siamese cat as sushi chef
43. With the style of Egyptian tomp hieroglyphics, A colossal gorilla in a force field armor defends a space colony.
44. a moose with the style of Hokusai
45. a cartoon pig playing his guitar, Andrew Warhol style
46. A cat watching the starry night by Vincent Van Gogh, Highly Detailed, 2K with the style of emoji
47. impressionist style, a yellow rubber duck floating on the wave on the sunset
48. A Egyptian tomp hieroglyphics painting ofA regal lion, decked out in a jeweled crown, surveys his kingdom.
49. Macro len style, A tiny mouse in a dainty dress holds a parasol to shield from the sun.
50. A young woman with blonde hair, blue eyes, and a prominent nose stands at a bus stop in a red coat, checking her phone. in the style of Anime, anime style
51. pikachu jedi, film realistic, red sword in renaissance style style
52. abstract cubism style, Freckles dot the girl's cheeks as she grins playfully
53. Howard Hodgkin style, A couple walks hand in hand along a beach, watching the sunset as they talk about their future together.
54. A horse sitting on an astronaut's shoulders. in Andrew Warhol style



“Iron Man is walking towards the camera in the rain at night, with a lot of fog behind him.”

“A cute happy Corgi playing in park, sunset, 4k.”

“A car moving slowly on an empty street, rainy evening, van Gogh painting.”

“A dog swimming in the river.”

Figure 9: **Qualitative experiments.** Under the FancyVideo framework, we train the **Video Extending** models, which includes extending videos forward and extending videos backward. In the forward expansion model, the input consists of 4 frames in red border, and the output is the subsequent 4 frames. With two iterations, we extend a 4-frame video to 12 frames. **In the backward expansion model**, the input consists of 4 frames, and the output is the subsequent 4 frames. With two iterations, we extend a 4-frame video to 12 frames. Similarly, **in the backward expansion model**, the input consists of 4 frames in red border, and the output is the preceding 4 frames. We also perform two iterations.

55. With the style of Howard Hodgkin, a woman with sunglasses and red hair
56. The old man the boat. in watercolor style
57. One morning I chased an elephant in my pajamas, Disney movie style
58. A rainbow arched across the sky, adding a burst of color to the green meadow. in Egyptian tomp hieroglyphics style
59. In Roy Lichtenstein style, In the video, a serene waterfall cascades down a rocky terrain. The water flows gently, creating a peaceful ambiance.
60. The night is dark and quiet. Only the dim light of street-lamps illuminates the deserted street. The camera slowly pans across the empty road. with the style of da Vinci
61. New York Skyline with 'Hello World' written with fireworks on the sky. in anime style
62. A car on the left of a bus., oil painting style
63. traditional Chinese painting style, a pickup truck at the beach at sunrise
64. a sword, Disney movie style
65. a statue with the style of van gogh
66. orange and white cat., slow motion
67. slow motion, A brown bird and a blue bear.
68. Two elephants are playing on the beach and enjoying a delicious beef stroganoff meal., camera rotate anticlockwise
69. camera pan from right to left, A trio of powerful grizzly bears fishes for salmon in the rushing waters of Alaska
70. a Triceratops charging down a hill, camera pan from left to right
71. hand-held camera, A real life photography of super mario, 8k Ultra HD.
72. drove viewpoint, a man wearing sunglasses and business suit
73. a girl with long curly blonde hair and sunglasses, camera pan from left to right
74. close-up shot, high detailed, a girl with long curly blonde hair and sunglasses
75. an old man with a long grey beard and green eyes, camera rotate anticlockwise
76. camera pan from left to right, a smiling man
77. drove viewpoint, fireworks above the Parthenon
78. zoom in, A serene river flowing gently under a rustic wooden bridge.
79. large motion, a flag with a dinosaur on it
80. still camera, an F1 race car



Figure 10: **Qualitative comparisons** of w CTGM and w/o CTGM in our method. In the solid red box on the left, unnatural stillness is apparent. Meanwhile, there is distortion in the red dashed box on the right. In the setting with CTGM, the above issues are resolved.

81. hand-held camera, Three-quarters front view of a blue 1977 Corvette coming around a curve in a mountain road and looking over a green valley on a cloudy day.
82. drove viewpoint, wine bottles
83. a paranoid android freaking out and jumping into the air because it is surrounded by colorful Easter eggs, camera rotate anticlockwise
84. A traveler explores a scenic trail on the back of a sturdy mule, taking in the breathtaking views of the mountains.
85. A farmer drives a tractor through a vast field, tending to the crops with care and expertise.
86. A violinist moves her bow in a large motion sweep, creating a beautiful melody.
87. A swimmer dives into the water with a large motion splash, beginning a race.
88. A drummer hits the cymbals with a large motion crash, punctuating the music.
89. Slow motion raindrops fall gently from the sky, creating ripples in a puddle.
90. Slow motion leaves fall from a tree, swirling through the air.
91. Slow motion lightning illuminates the dark sky, followed by the rumble of thunder.
92. Slow motion bubbles rise to the surface of a glass of champagne.
93. Slow motion smoke curls up from a burning candle.

94. Slow motion confetti falls from the sky, celebrating a victory.
95. Slow motion steam rises from a hot cup of coffee.
96. Slow motion birds soar through the sky, their wings outstretched.
97. Three dogs playfully chase each other around a park.
98. Three horses gallop across a wide open field, tails and manes flying in the wind.
99. A blue boat sailing on the water with a red flag.
100. A person riding a green motorbike with an orange helmet.
101. A green cow grazing in a field with a yellow sun.
102. A yellow cat sleeping on a green bench.
103. Brad Pitt smirks charmingly, his blue eyes sparkling with mischief.
104. Angelina Jolie's full lips curve into a smile, her gaze intense and captivating.
105. Tom Cruise's intense stare conveys determination, his jaw set firmly.
106. Leonardo DiCaprio's eyes glimmer with passion, his handsome face displaying intensity.
107. Robert Downey Jr.'s smug grin conveys his character's confidence, his eyes full of wit.
108. Johnny Depp's face shows playfulness, his eyes twinkling with mischief.



Figure 11: **Qualitative analysis** of our approach to long video generation (64 frames). More results are shown in .

1024 × 768



“With the style of Howard Hodgkin, a woman with sunglasses and red hair.”



“The old man the boat. in watercolor style.”

768 × 1024



“A dog swimming in the river.”



“A cute and chubby giant panda is enjoying a bamboo meal in a lush forest.”

1024 × 1024



“A yellow rubber duck floating on the wave on the sunset.”



“A panda standing on a surfboard in the ocean in sunset.”

Figure 12: **Qualitative experiments.** By switching different base models, we demonstrate experimental results at multiple pixel scales.

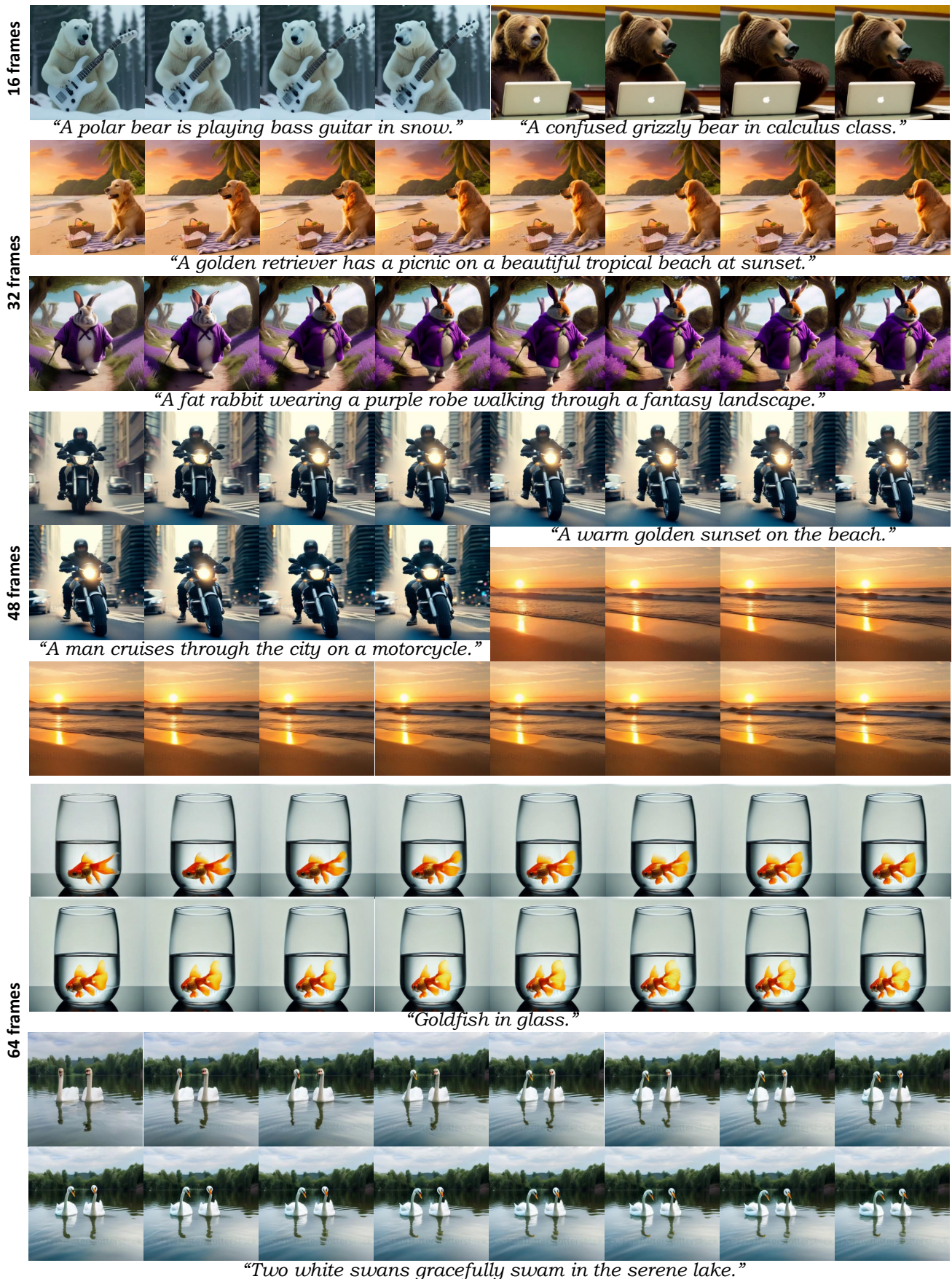


Figure 13: **Qualitative experiments.** We demonstrate the experimental results of FancyVideo with 16, 32, 48, and 64 frames.